Numerical Comparison of $Cu$and Al_2O_3 Nanoparticles in an MHD Water-based Nanofluid

Abstract

In this study, the impact of Cu and Al_2O_3nanoparticles in a water-based nanofluid are considered. The application of this can be found in biomedical sensors and drug delivery. Specifically, it investigates heat transfer in the MHD flow of two nanofluids (Cu-water and Al_2O_3-water) over an exponentially stretching surface. The study formulates a model and renders it dimensionless using Similarity Transformation. Numerical solutions are obtained using the MATLAB package bvp4c. The focus is on analysing the heat transfer rate variation with nanoparticle volume fraction. Results indicate that Cu-water nanofluid exhibits higher heat transfer rates and lower skin frictions compared to Al_2O_3-water nanofluid.

Keywords: Heat Transfer, MHD flow, hybrid nanofluid

Nomenclature

Symbol	Meaning	Symbol	Meaning
u, v, w	Velocity in the x, y, z-directions	μ_{nf}	effective nanofluid viscosity
T	Dimensional fluid temperature	μ_{bf}	base fluid viscosity
T_∞	free stream temperature	μ_{np}	nanoparticle viscosity
T_w	wall temperature	ρ_{nf}	effective nanofluid density
g^*	Acceleration due to gravity	ρ_{bf}	base fluid density
k^*	mean absorption coefficient	ρ_{np}	nanoparticle density
B_0	magnetic field strength	β	Coefficient of thermal expansion
c_p	Specific heat capacity	σ_{nf}	effective electrical conductivity
σ^*	Stefan–Boltzmann constant	k_{nf}	effective nanofluid thermal conductivity
ϕ	nanoparticle volume fraction	α_{nf}	effective nanofluid thermal diffusivity

1 Introduction

Maxwell [1] introduced the concept of enhancing thermal and electrical conductivity in fluids by incorporating solid particles. While initially successful, issues such as pipe clogging and erosion arose with the use of millimetre-sized particles. Choi and Eastman [2] proposed an alternative approach of dispersing nanoparticles in the fluid, termed nanofluids, which addressed these issues. Nanotechnology advancements have since facilitated significant progress in nanofluid preparation and application, particularly in engineering and industrial sectors. Nanofluids find utility in diverse areas, including oil well recovery [3], waste heat retrieval [4], and cooling systems for microchips and car radiators [5-7].

Additionally, when fluid flow occurs under magnetic influence, both thermal and electrical properties are further enhanced. The magnetohydrodynamic flow of nanofluids has garnered global attention, particularly for its applications in micro-technology advancement. Due to the complexity and resource-intensive nature of nanofluid preparation, theoretical and numerical studies are preferred over experimental approaches. Consequently, there is a greater emphasis on theoretical investigations of magnetohydrodynamic nanofluid flow compared to experimental research [8-10].

The passage of a fluid with electrical conductivity in a magnetic field induces an electric current, resulting in a loop of magnetic field generation. This phenomenon, known as magnetohydrodynamic (MHD) flow, is significant in various fields, such as biomedical applications,

astrophysics, and liquid metal flows. Nayak et al. [11] investigated free convective MHD flow with varying magnetic field strength in three nanofluids based on different base fluids, comparing heat transfer rates and skin friction. Elazem [12] numerically explored the effect of magnetic field strength on nanofluid flow when a plate is linearly stretched, focusing on heat and mass transfer rates. Irfan et al. [13] analysed the impact of time-dependent viscosity, thermal conductivity, surface stretching, and wall temperature on MHD nanofluid flow thermophysical properties. Noor et al. [14] studied the MHD flow of Jeffrey nanofluids, emphasising volume fraction effects rather than nanoparticle material. Results showed that increasing magnetic field intensity slowed down the flow, consistent with previous studies. Ahmed and Akbar [15] investigated the MHD flow of Williamson nanofluid over an ESS. Haroon et al. [16] examined the effects of uniform magnetism and heat radiation on nanofluid flow, noting that magnetism impedes fluid flow. Atif et al. [17] considered a micropolar-based nanofluid with thermal radiation and mixed convection, finding that magnetic field presence enhances flow temperature.

This study analyses the MHD flow of water-based nanofluids over an exponentially stretching surface in three dimensions, focusing on the effects of nanoparticle material and volume fraction. Specifically, the study compares the flow characteristics of two conducting nanofluids: $Cu - H_2O$ and $Al_2O_3 - H_2O$nanofluids. By varying the volume fraction of nanoparticles, the project seeks to investigate the rate of heat transfer. The significance of using Cu and Al_2O_3The nanoparticle in the MHD flow of water-based nanofluid over an Exponentially stressing surface will be examined, shedding light on the impact of nanoparticle material and volume fraction on flow parameters.

2 Methodology

2.1 Governing Equations

The flow configuration depicted in Figure (1) illustrates a steady, three-dimensional flow, with the magnetic field oriented along the z-axis. The nanofluid flows within the x-y plane, influenced by magnetisation perpendicular to the flow plane. In accordance with the steady nature of the flow, the continuity equation can be expressed as:

$$\frac{\partial u}{\partial x}+\frac{\partial v}{\partial y}+\frac{\partial w}{\partial z}=0. \tag{1}$$

and the momentum and energy equations are

$$u\frac{\partial u}{\partial x}+v\frac{\partial u}{\partial y}+w\frac{\partial u}{\partial z}=\frac{\mu_{nf}}{\rho_{nf}}\frac{\partial^2 u}{\partial z^2}+g^*\beta(T-T_\infty)-\frac{\sigma_{nf}B_0^2 u}{\rho_{nf}} \tag{2}$$

$$u\frac{\partial v}{\partial x}+v\frac{\partial v}{\partial y}+w\frac{\partial v}{\partial z}=\frac{\mu_{nf}}{\rho_{nf}}\frac{\partial^2 w}{\partial y^2}+g^*\beta(T-T_\infty)+\frac{\sigma_{nf}B_0^2 v}{\rho_{nf}} \tag{3}$$

$$u\frac{\partial T}{\partial x}+v\frac{\partial T}{\partial y}+w\frac{\partial T}{\partial z}=\left(\alpha_{nf}+\frac{16\sigma^* T_\infty^3}{3k^*\left(\rho c_p\right)_{nf}}\right)\frac{\partial^2 T}{\partial z^2}, \tag{4}$$

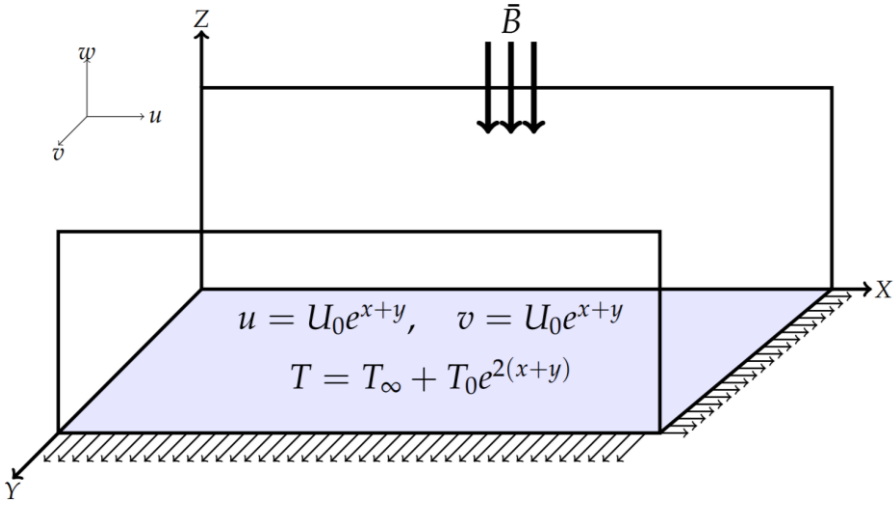

Fig. **1.** Pattern of flow

The effective dynamic viscosity, density, thermal diffusivity and heat capacity are defined in [18 - 21] as

$$\mu_{nf} = (1 + 7.3\phi + 123\phi^2)\mu_{bf}, \quad \rho_{nf} = (1-\phi)\rho_{bf} + \phi\rho_{np}, \tag{5}$$

$$\alpha_{nf} = \frac{k_{nf}}{(\rho c_p)_{nf}}, (\rho c_p)_{nf} = (\rho c_p)_{bf}\left(1 - \phi + \phi\frac{(\rho c_p)_{np}}{(\rho c_p)_{bf}}\right) \tag{6}$$

$$k_{nf} = k_{bf}k_{np}\left[2\frac{k_{bf}}{k_{np}} + \frac{\phi}{k_{np}}(k_{bf} - k_{np}) + k_{np} + 2k_{bf} - 2\phi(k_{bf} - k_{np})\right]. \tag{7}$$

The BCs are

$$at \;\; z = 0; \quad u = v = U_0\exp(x+y), \quad w = 0, \quad T = T_\infty + T_0\exp(2x+2y) \tag{8}$$

$$as\; z \to \infty; \quad u \to 0, \quad v \to 0, \quad T \to T_\infty \tag{9}$$

Factors of engineering applications are the skin friction and heat transfer rates;

$$Cf_x = \frac{\tau_x}{\rho_{nf}U_w^2}, \quad Cf_z = \frac{\tau_y}{\rho_{nf}U_w^2}, \text{and} \quad Nu = \frac{zq_w}{\kappa_{nf}(T_w - T_\infty)}. \tag{10}$$

respectively, where the shear stress τ is

$$\tau_x = \mu_{nf}\left.\frac{\partial u}{\partial z}\right|_{z=0} \quad and \quad \tau_z = \mu_{nf}\left.\frac{\partial v}{\partial z}\right|_{z=0}. \tag{11}$$

and the heat flux q_w is

$$q_w = -\kappa_{nf}\left.\frac{\partial T}{\partial y}\right|_{z=0}. \tag{12}$$

*2.2 **Nondimensionalisation***

The similarity variables

$$\eta = \left(\frac{U_0}{2\nu_{bf}}\right)^{\frac{1}{2}} z\exp\left(\frac{x+y}{2}\right), \quad u = U_0 f'\exp(x+y), v = U_0 g'\exp(x+y), \tag{13}$$

$$w = -\left(\frac{\nu_{bf}U_0}{2}\right)^{\frac{1}{2}}(f + \eta f' + g + \eta g')\exp\left(\frac{x+y}{2}\right), \quad T = T_\infty + \theta T_0\exp(2x+2y) \tag{14}$$

With these variables, the system reduces to

$$A_1 f''' + 2Gr\theta - 2Mf' - 2f'(f' + g') + f''(f+g) = 0, \tag{15}$$

$$A_1 g''' + 2Gr\theta + 2Mg' - 2g'(f' + g') + g''(f + g) = 0, (16)$$
$$\left(1 + \frac{4}{3}R\right) A_2 \theta'' - 4Pr\theta(f' + g') + Pr(f + g)\theta' = 0. \quad (17)$$

with the initial and BCs

$$f' = 1; g' = 1; 0 = f + g; \ \theta = 1; \quad at \ \ \eta = 0, \quad (18)$$

$$f' = 0; g' = 0; \ \theta = 0; \quad as \ \ \eta \to \infty. \quad (19)$$

where

$$A_1 = \frac{(1 + 7.3\phi + 123\phi^2)}{\left(1 - \phi + \phi\frac{\rho_{np}}{\rho_{bf}}\right)}, Gr = \frac{g^*\beta T_0}{U_0^2}, \quad M = \frac{\sigma_{nf} B_0^2}{U_0 \rho_{nf} e^{x+y}}, Pr = \frac{\nu_{bf}}{\alpha_{bf}}, \qquad R = \frac{4\sigma^* T_\infty^3}{k^*(\rho c_p)_{nf} \alpha_{nf}}.$$

The quantities of engineering interests are;

$$Re^{-\frac{1}{2}} Cf_x = A_1 f''(0), \qquad Re^{-\frac{1}{2}} Cf_y = A_1 g''(0), Re^{\frac{1}{2}} Nu = \theta'(0) (20)$$

*2.3 **Numerical Method***

By rewriting

$$H_1 = f, H_2 = f', H_3 = f'',$$
$$H_4 = g, H_5 = g', H_6 = g'',$$
$$H_7 = \theta, H_8 = \theta',$$

equations (21) – (23) are put as a system of 1st-order ODEs

$$H_1' = H_2, H_2' = H_3, \ H_3' = -\frac{1}{A_1}\left(2GrH_7 - 2MH_2 - 2H_2(H_2 + H_5) + H_3(H_1 + H_4)\right),$$
$$H_4' = H_5, \ H_5' = H_6, \ H_6' = -\frac{1}{A_1}\left(2GrH_7 + 2MH_5 - 2H_5(H_2 + H_5) + H_6(H_1 + H_4)\right),$$
$$H_7' = H_8, \ H_8' = -\frac{1}{\left(1 + \frac{4}{3}R\right)A_2}(-4PrH_4(H_2 + H_5) + Pr(H_2 + H_4)H_8).$$

with the conditions

$$H_2(0) = 1; H_5(0) = 1; H_1(0) + H_4(0) = 0; H_7(0) = 1;$$
$$H_2(\infty) = 0; H_5(\infty) = 0; H_7(\infty) = 0.$$

The Shooting technique with the Runge-Kutta method is adopted in solving this system [22].

3 Results and Discussion

The investigation of heat transfer rates and skin friction for copper-water and alumina-water nanofluids is depicted graphically in figures (2) and (3). In both figures, the black lines represent copper-water nanofluid, while the blue lines represent alumina-water nanofluid. Each nanofluid is examined under two conditions: low thermal radiation and high thermal radiation. Figure (2) illustrates that heat transfer rates increase with thermal radiation, with copper-water nanofluid exhibiting higher heat transfer rates compared to alumina-water nanofluid. This difference can be attributed to the higher specific heat of alumina nanoparticles compared to copper nanoparticles.

Regarding skin friction, it is low at low thermal radiation for both nanofluids but increases at high thermal radiation (see Figure 3). Further analysis of Figure (3) reveals that skin friction is higher during alumina-water nanofluid flow compared to copper-water flow. Consequently, while the heat

transfer rate is higher in Cu-H_2O nanofluid compared to Al_2O_3-H_2O nanofluid, skin friction is higher in Al_2O_3-H_2O than in Cu-H_2O.

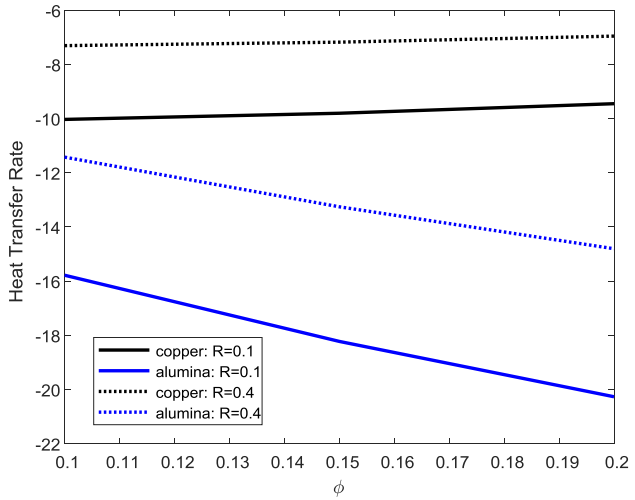

Fig. 2. Nu against ϕ at low and high thermal radiation

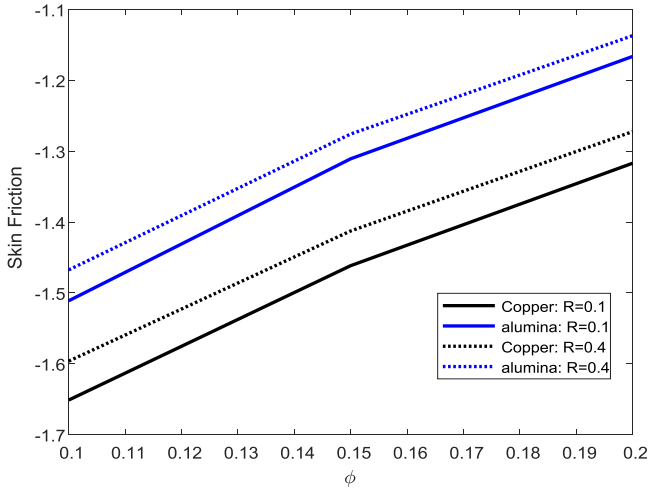

Fig. 3. Cf against ϕ at lowandhighthermal radiation

Volume fraction refers to the ratio of the volume of copper or alumina nanoparticles suspended in a specific volume of water. Figures (4) and (5) analyse the flow response by varying the volume fraction (ϕ). It is important to note that suspending a higher volume of nanoparticles in the fluid can lead to aggregation, which may cause wear on pipe linings. Due to the lower density of alumina nanoparticles compared to copper nanoparticles, the flow velocity is higher in the Al_2O_3-H_2O nanofluid than in the copper-water nanofluid, as depicted in Figures (4). Additionally, upon closer examination of Figures (4), it can be generally inferred that flow velocity increases as the volume fraction increases. However, flow temperature decreases as more volume fraction of nanoparticles are suspended in the base fluid, as shown in Figure (5).

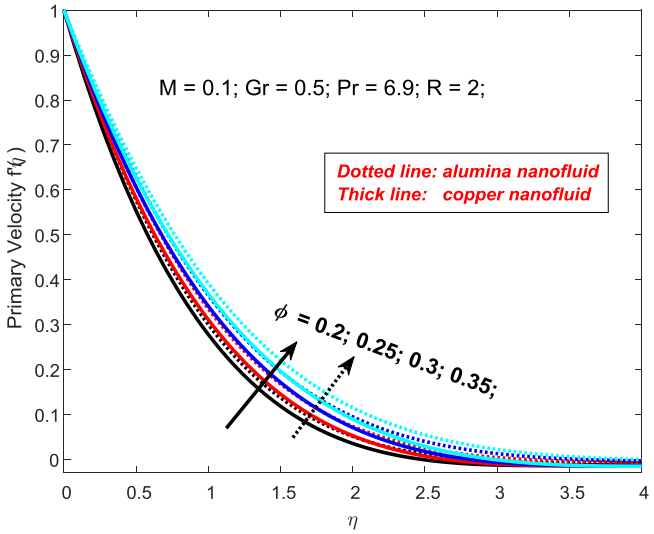

Fig. 4. Primary velocity against ϕ

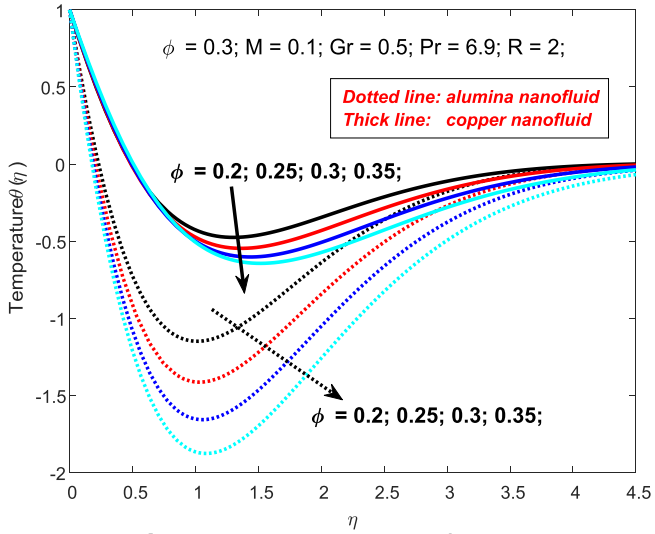

Fig. 5. Temperature against ϕ

The effects of magnetic field strength on the flow of copper-water and alumina-water nanofluids are analysed, with results depicted in figures (6) and (7). It's essential to note that Lorenz force is generated when flow occurs in a magnetic field, acting against the flow and thereby reducing velocity as the magnitude of the magnetic field strength increases. As expected, the velocity profile decreases with increasing magnetic field strength, as illustrated in Figure (6). Additionally, from Figure (6), it's observed that the alumina-water nanofluid flows at a higher velocity than the Cu-H_2O nanofluid. Moreover, the Al2O3-H2O nanofluid exhibits a higher flow temperature compared to the

Cu-H_2O nanofluid, as depicted in Figure (7).

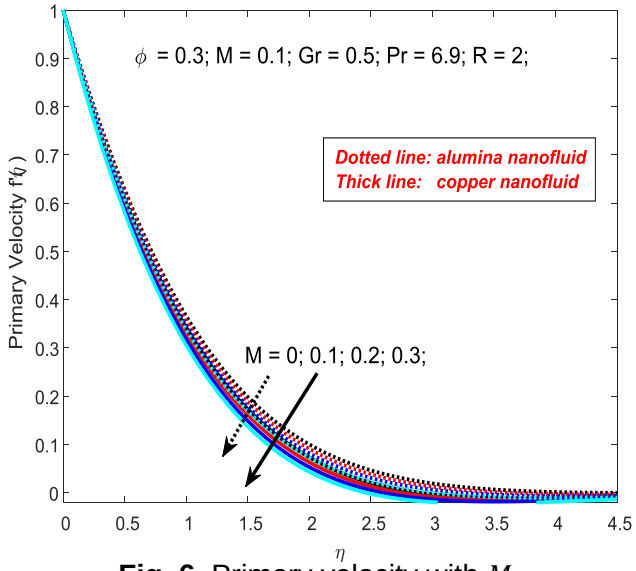

Fig. 6. Primary velocity with M

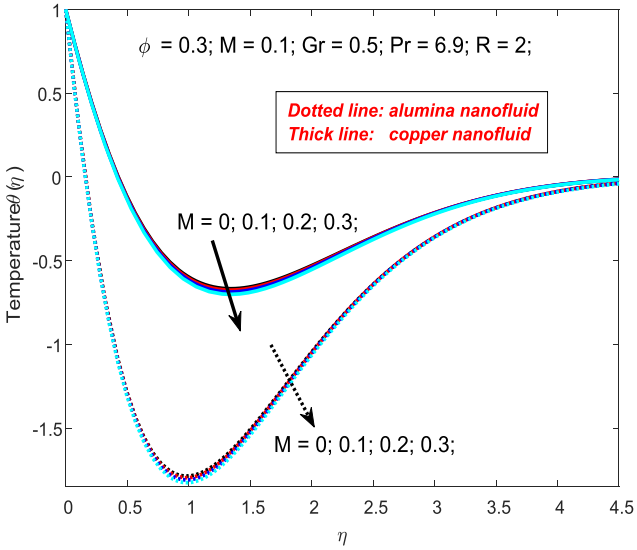

Fig. 7. Temperature with M

4 Conclusion

The project analysestheheattransmission during the flow of copper-water and alumina-water nanofluids in a magnetic field. The surface undergoes horizontal exponential stretching while thermal radiation is applied perpendicular to the flow. Mathematical equations are reformulated dimensionally and solved using the RK4-Sh method. The outcomes of the study reveal the following:

1. Heat transfer rates increase with thermal radiation, with copper-water nanofluid exhibiting higher rates compared to alumina-water nanofluid.

2. Skin friction increases with thermal radiation, with alumina-water nanofluid demonstrating higher friction compared to copper-water nanofluid.

3. Flow velocity is enhanced as the volume fraction increases, with alumina-water nanofluid exhibiting higher velocity.

4. Flow temperature decreases with increasing volume fraction of nanoparticles in the base fluid.

References

[1] Maxwell, J. C. (1873). A Treatise on Electricity and Magnetism. *Nature*, 7:478–480.

[2] Choi, S. U. S. and Eastman, J. A. (1995). Enhancing Thermal Conductivity of Fluids with Nanoparticles. *ASME International Mechanical Engineering Congress & Exposition*.

[3] McElfresh, P., Holcomb, D., and Ector, D. (2012). Application of Nanofluid Technology to Improve Recovery in Oil and Gas Wells. *SPE International Oilfield Nanotechnology Conference and Exhibition*. SPE-154827-MS.

[4] Olabi, A. G., Elsaid, K., Sayed, E. T., Mahmoud, M. S., Wilberforce, T., Hassiba, R. J., and Abdelkareem, M. A. (2021). Application of nanofluids for enhanced waste heat recovery: A review. *Nano Energy*, 84:105871.

[5] Oke, A. S., Animasaun, I. L., Mutuku, W. N., Kimathi, M., Shah, N. A., and Saleem, S. (2021). Significance of Coriolis force, volume fraction, and heat source/sink on the dynamics of water conveying 47nm alumina nanoparticles over a uniform surface.

Chinese Journal of Physics, 71:716–727.
[6] Oke, A. S. (2022). Combined effects of Coriolis force and nanoparticle properties on the dynamics of gold–water nanofluid across nonuniform surface. *ZAMM - Journal of Applied Mathematics and Mechanics/Zeitschrift für Angewandte Mathematik und Mechanik*, *102*(9), e202100113.
[7] Animasaun, I. L., Oke, A. S., Al-Mdallal, Q. M., & Zidan, A. M. (2023). Exploration of water conveying carbon nanotubes, graphene, and copper nanoparticles on impermeable stagnant and moveable walls experiencing variable temperature: Thermal analysis. *Journal of Thermal Analysis and Calorimetry*, *148*(10), 4513-4522.
[8] Malia, M. and Chepkwony, I. (2019). Effects on temperature on applying variable pressure gradient to a magnetohydrodynamic fluid flowing between plates with inclined magnetic field. *Mathematical Theory and Modeling*, 9(11):45–56.
[9] Oke, A. S., Fatunmbi, E. O., Animasaun, I. L., & Juma, B. A. (2022). Exploration of ternary-hybrid nanofluid experiencing Coriolis and Lorentz forces: case of three-dimensional flow of water conveying carbon nanotubes, graphene, and alumina nanoparticles. *Waves in Random and Complex Media*, 1-20.
[10] Oke, A. S., Prasannakumara, B. C., Mutuku, W. N., Gowda, R. P., Juma, B. A., Kumar, R. N., & Bada, O. I. (2022). Exploration of the effects of Coriolis force and thermal radiation on water-based hybrid nanofluid flow over an exponentially stretching plate. *Scientific Reports*, *12*(1), 21733.
[11] Nayak, M. K., Shaw, S., and Chamkha, A. J. (2019). 3D MHD Free Convective Stretched
[12] Abd Elazem, N. Y. (2021). Numerical results for influence the flow of MHD nanofluids on heat and mass transfer past a stretched surface. *Nonlinear Engineering*, *10*(1), 28-38.
[13] Irfan, M., Farooq, M. A., Aslam, A., Mushtaq, A., & Shamsi, Z. H. (2021). Magnetohydrodynamic time-dependent bio-nanofluid flow in a porous medium with variable thermophysical properties. *Mathematical Problems in Engineering*, *2021*, 1-16.
[14] Mat Noor, N. A., Shafie, S., & Admon, M. A. (2021). Heat and mass transfer on MHD squeezing flow of Jeffrey nanofluid in horizontal channel through permeable medium. *Plos one*, *16*(5), e0250402.
[15] Ahmed, K., & Akbar, T. (2021). Numerical investigation of magnetohydrodynamics Williamson nanofluid flow over an exponentially stretching surface. *Advances in Mechanical Engineering*, *13*(5), 16878140211019875.
[16] Rasheed, H. U., Islam, S., Khan, Z., Alharbi, S. O., Alotaibi, H., & Khan, I. (2021). Impact of nanofluid flow over an elongated moving surface with a uniform hydromagnetic field and nonlinear heat reservoir. *Complexity*, *2021*, 1-9.
[17] Atif, S. M., Abbas, M., Rashid, U., and Emadifar, H. (2021). Stagnation Point Flow of EMHD Micropolar Nanofluid with Mixed Convection and Slip Boundary. *Complexity*, 2021(Article ID 3754922).
[18] Oke, A. S. (2021). Coriolis effects on MHD flow of MEP fluid over a non-uniform surface in the presence of thermal radiation. *International Communications in Heat and Mass Transfer*, *129*, 105695.
[19] Oke, A. S. (2022). Theoretical analysis of modified Eyring Powell fluid flow. *Journal of the Taiwan Institute of Chemical Engineers*, *132*, 104152.
[20] Oke, A. S., Mutuku, W. N., Kimathi, M., & Animasaun, I. L. (2021). Coriolis effects on MHD Newtonian flow over a rotating non-uniform surface. *Proceedings of the Institution of Mechanical Engineers, Part C: Journal of Mechanical Engineering Science*, *235*(19), 3875-3887.
[21] Oke, A. S. (2022). Heat and mass transfer in 3D MHD flow of EG-based ternary hybrid nanofluid over a rotating surface. *Arabian Journal for Science and Engineering*, *47*(12), 16015-16031.
[22] Oke, A. S. (2017). Convergence of differential transform method for ordinary differential equations. *Journal of Advances in Mathematics and Computer Science*, *24*(6), 1-17.